Retrovirus-Based Virus-Like Particle Immunogenicity and Its Modulation by Toll-Like Receptor Activation

Fabien Pitoiset, Thomas Vazquez, Béatrice Levacher, Djamel Nehar-Belaid, Nicolas Derian, James Vigneron, David Klatzmann, Bertrand Bellier

Retrovirus-based Virus-Like Particle Immunogenicity and its Modulation by Toll-Like Receptor Activation

Fabien Pitoiset [a, b], Thomas Vazquez [a, b], Beatrice Levacher [a, b, *], Djamel Nehar-Belaid [a, b, *], Nicolas Dérian [a, b], James Vigneron [a, b], David Klatzmann [a, b, c], Bertrand Bellier [a, b, c, #].

[a] Sorbonne Universités, UPMC Univ Paris 06, UMRS_959, I^3, Paris, France

[b] INSERM, UMR_S 959, Paris, France

[c] AP-HP, Groupe Hospitalier Pitié-Salpêtrière, Department of Biotherapies and the Clinical Investigation Center in Biotherapy, Paris, France

* Authorship equal contribution

Running Title: Improvement of retrovirus-derived VLP immunogenicity by TLR ligand

Address correspondence to Bertrand Bellier: bertrand.bellier@upmc.fr

Word counts: abstract: 180 words, importance: 121 words, text: 5434 words.

Abstract

Retrovirus-derived virus-like particles (VLPs) are particularly interesting vaccine platforms as they trigger efficient humoral and cellular immune responses and can be used to display heterologous antigens. In this study, we characterized the intrinsic immunogenicity of VLPs and investigated their possible adjuvantization by incorporation of toll-like receptor (TLR) ligands. We designed a non-coding single-stranded RNA (ncRNA) that could be encapsidated by VLPs and induce TLR7/8-signaling. We found that VLPs efficiently induce *in vitro* dendritic cell activation, which can be improved by ncRNA encapsidation ($_{ncRNA}$VLPs). Transcriptome studies of dendritic cells harvested from the spleen of immunized mice identified antigen presentation and immune activation as the main gene expression signatures induced by VLPs, while TLR signaling and Th1 signatures characterize $_{ncRNA}$VLPs. *In vivo* and compared with standard VLPs, $_{ncRNA}$VLPs promoted Th1 responses and improved CD8+ T cell proliferation in a MyD88-dependent manner. In an HIV vaccine mouse model, HIV-pseudotyped $_{ncRNA}$VLPs elicited stronger antigen-specific cellular and humoral responses than VLPs. Altogether our findings provide molecular evidence for a strong vaccine potential of retrovirus-derived VLPs that can be further improved by harnessing TLR-mediated immune activation.

Importance

We previously reported that DNA vaccines encoding antigens displayed in/on retroviral VLPs are more efficient than standard DNA vaccines at inducing cellular and humoral immune responses. We aimed to decipher the mechanisms and investigated the VLPs immunogenicity independently of the DNA vaccination. We show that VLPs have the ability to activate antigen-presenting cells directly, thus confirming their intrinsic immunostimulatory properties and their potential to be used as an antigenic platform. Notably, this immunogenicity can be further improved and/or oriented by the incorporation into VLPs of ncRNA, which provides further TLR-mediated activation and Th1-type CD4+ and CD8+ T cell response orientation. Our results highlight the versatility of retrovirus–derived VLP design and the value of using ncRNA as an intrinsic vaccine adjuvant.

Introduction

The development of successful vaccines against viruses such as HIV or HCV requires new approaches, and in particular vaccines that are able to elicit both cellular and humoral immune responses contributing to protective immunity. A major advance in vaccine development has been the production of antigens as virus-like particles (VLPs) that mimic the overall structure of virus particles, without the requirement of containing infectious genetic material. VLP designs are based on the observation that expression of the capsid proteins of many viruses leads to the spontaneous assembly of pseudo-particles with an authentic conformation, but devoid of DNA or RNA viral genome, thus rendering them replication incompetent. In addition to safety, their particulate nature, highly repetitive structure and ability to activate innate immune cells explain the strong immunogenicity of VLPs (1),(2) and their success in vaccine development (3). To date, VLPs have been used as prophylactic vaccines against homologous viral diseases, such as hepatitis B or papillomavirus infection, and have shown excellent efficacy and safety profiles. VLPs have also been proposed as an antigen carrier platform for heterologous vaccination. The insertion of target antigens into viral structural proteins able to self-assemble has been the most common method of producing these chimeric VLPs. Different VLPs have been adapted for this purpose (4) and there have been notable successes in developing vaccines, notably against malaria (5).

We previously developed recombinant murine leukemia retrovirus–based VLPs (MLV VLPs) as a vaccine platform. These VLPs are made of the Moloney MLV-Gag capsid proteins that can self-assemble into pseudo-particles in host cells by budding at the plasma membrane. Target antigens can be inserted either into the particles by fusion with Gag proteins or displayed at their surface by co-expression of Gag with recombinant protein fused to the transmembrane domain of the vesicular stomatitis virus glycoprotein (VSV-G) (6). We demonstrated that the expression of antigens both in and on VLPs significantly improves their immunogenicity, favoring the induction of both B- and T-cell–mediated immunity in a context of DNA vaccination. Indeed, plasmid DNA encoding chimeric VLPs induces higher cellular and humoral immune responses against target antigens than a control DNA vaccine encoding antigens not associated with VLPs (7),(8),(9),(10).

In order to favor vaccine-induced Th1 responses, which play a critical role in antiviral immunity (11),(12), stimulation of Toll-like receptor (TLR) ligands (13) has been investigated (14). TLRs are receptors expressed by innate immune cells, predominantly by antigen-presenting cells (APCs), and recognize various pathogen components, such as proteins, nucleic acids or sugars, from viruses, bacteria or parasites (15). Upon binding to pathogen-associated molecular patterns (PAMPs), TLR signaling activates the APCs resulting in production by dendritic cells (DCs) of cytokines, notably IL-6, IL-12 and IFN-γ (14), increased co-stimulatory molecule expression and enhanced capacity to present and cross-present antigens on MHC class I molecules (16),(17). Among the different TLRs that are able to recognize pathogenic nucleic acids, TLR7, 8 and 9 have been extensively studied for the induction of Th1 responses for anti-tumor and anti-viral vaccination (17),(18),(19),(20).

Here, we designed a new strategy to incorporate non-coding RNA (ncRNA), which acts as a TLR7/8 ligand in MLV-derived VLPs and is characterized by its impact on their immune properties. We compared VLPs and $_{ncRNA}$VLPs for their capacity to activate DCs, to prime CD8+ and CD4+ T cell responses and to generate anti-HIV immune responses in mice. Collectively, our results demonstrate that MLV-derived VLPs have intrinsic adjuvant properties that can be further improved by incorporation of ncRNA.

Material and Methods

Cell lines

HEK293T cells (CRL-1573; ATCC) were grown in Dulbecco's modified Eagle medium (DMEM) supplemented with 2 mM L-glutamine, 100 U/mL penicillin, 100 µg/mL streptomycin (all from Life Technologies, Cergy Pontoise, France) and 10% heat-inactivated fetal calf serum.

Mice

6- to 7-week-old female C57BL/6J mice were from Janvier Labs (Le Genest-Saint-Isle, France). OT-I (C57BL/6-Tg(TcraTcrb)1100Mjb), OT-II (C57BL/6-Tg(TcraTcrb)425Cbn) and MyD88$^{-/-}$ (on a C57BL/6 background; (21)) mice were bred

at the CEF animal facility at the Pitié-Salpêtrière Hospital. Mice were maintained under specific pathogen-free conditions, and manipulations were performed according to European Economic Community guidelines and approved by the local ethics committee (ce5/2009/042).

Plasmid DNA

pGag encodes the Moloney MLV-Gag under the CMV promoter. pGag is obtained by deletion of Pol by PCR in the pBL35 (7) with insertion of the MluI restriction site at the 3' end of Gag before the terminal stop amino acid. For pGag-gp33-41, the KAVYNFATC epitope (gp33-41), flanked upstream and downstream by 5 natively neighboring amino acids as previously described (7), was added at the 3' end of the MLV gag sequence in pGag. pBL196 encodes a fusion protein MLV-Gag-OVA. The OVA sequence was synthesized (GenScript Corporation, Piscataway, NJ 08854, USA) and inserted at the end of MLV-Gag with restriction sites (MluI/XbaI) in pGag. phCMV-VSV-G encoding VSV-G was previously described (22). pgp140-TM is a synthetic plasmid under the EF1α promoter encoding the $GP140_{TM}$ fusion chimeric protein. HIV Gp140 (Clade B, Strain JRFL) was fused after Lys-674 to the VSV-G transmembrane domain (TM) by PCR insertion of the 49 amino acids from Ser-463 to Lys-511. pncRNA was obtained by deleting the coding region from a CMV-GFP retroviral transgene (kindly provided by FL Cosset) after digestion with EcoR1.

Production of VLPs

HEK-293T cells (ATCC/CRL-1573) (15×10^6 cells/175 cm^2 flask) were transfected using a calcium phosphate protocol with 50 µg of total plasmid DNA. For VLPs (i) pGag and phCMV-VSV-G or (ii) pGag-gp33-41 and pgp140-TM were used in a 2:1 ratio. For $_{ncRNA}$VLPs (i) pGag, phCMV-VSV-G and pncRNA or (ii) pGag-gp33-41, pgp140-TM and pncRNA were used in a 2:1:1 ratio. After 48 h, supernatants were collected, filtered through 0.45 µm pore-sized membranes and concentrated with Centricon (Millipore, Molsheim, France). Then, supernatants were layered on top of a sucrose step gradient (2.5 mL 35% and 2.5 mL 50%) and centrifuged at 100,000 g for 2 h at 4°C. The interface was collected and washed with PBS in an identical centrifugation step to eliminate remaining sucrose. Quantification of VLPs was performed by BCA (Thermo Fisher Scientific, USA).

Endotoxin quantification

Endotoxin levels in VLP preparations were quantified with the LAL Chromogenic Endotoxin Quantitation Kit (Thermo Fisher Scientific), following manufacturer's instructions. Absorbance was read at a wavelength of 405 nm in a DTX-800 Microplate Reader (Beckman Coulter, USA).

Detection of ncRNA in VLPs

Purified VLPs and $_{ncRNA}$VLPs were incubated at 75°C for 10 min to release RNA and treated with DNase I RNase-free (Invitrogen, France) for 30 min at room temperature. As a control, total RNA from HEK-293T cells (3.10^6 cells) was isolated by using RNeasy Mini Kits (Qiagen, France). cDNA synthesis from HEK-293T or VLPs was performed in triplicate using Superscript III (Invitrogen, France) according to the manufacturer's instructions, using primers specific to the MLV LTR region. Forward primer 5′- ATA GAC TGA GTC GCC CGG-3′ and reverse primer 5′- AGC GAG ACC ACA AGT CGG AT-3′ were synthesized by Sigma-Aldrich. Quantitative PCR was performed using the 7500 Fast Real-Time PCR System (Life Technologies, France) with FG, Power Sybr master mix (Life Technologies, France).

Quantification of total RNA in VLPs

VLPs were transfered in Trizol Reagent (Life Technologies, France) and extraction was performed according to the manufacturer's instructions. Phase Lock Gel (5PRIME) was used to separate phases. Extracted RNA was treated with the DNA-free Kit (Ambion). Yields of RNA from VLPs were determined by the Quant-iT™ RiboGreen RNA Reagent (Invitrogen). Escherichia coli 16S and 23S rRNA provided by the manufacturer were used as controls.

Assay of murine bone marrow–derived dendritic cell activation

Bone marrow cells collected from tibias and femurs of C57Bl/6 or MyD88$^{-/-}$ mice were cultured for 9 days in IMDM medium (Life Technologies, Cergy Pontoise, France) supplemented with 2 mM L-glutamine, 100 U/mL penicillin, 100 µg/mL streptomycin (all from Life Technologies, Cergy Pontoise, France), 10% heat-inactivated fetal calf serum and GM-CSF (supernatant of J558 hybridoma kindly provided by D. Gray, University of Edinburgh, Edinburgh, U.K.). Fresh medium was added every 3 days.

At day 9, differentiated BMDCs were cultured for 24 additional hours in the presence of VLPs, $_{ncRNA}$VLPs or medium alone as control. Expression of activation markers was analyzed by flow cytometry.

Transcriptome analysis of dendritic cells

C57Bl/6 mice were i.v. injected with 25 µg of VSV-G-pseudotyped VLPs, $_{ncRNA}$VLPs or with PBS in the control group. Six hours later the mice were sacrificed and DCs were isolated from spleen using magnetic separation with CD11c-specific microbeads (Miltenyi Biotec, Paris, France). Purity of sorting cells was verified by flow cytometry and cells were frozen in Trizol after 2 washes in PBS. RNA was isolated using the RNeasy Mini kit (QIAGEN). RNA yield was assessed using a NanoDrop ND-1000 spectrophotometer (Thermo Fisher Scientific) and RNA integrity was confirmed by using an Agilent Bioanalyzer (Agilent Technologies) with a minimum RNA integrity number (RIN) of 9. Total RNA was amplified and converted to biotinylated cRNA according to the manufacturer's protocol (Illumina TotalPrep RNA Amplification Kit; Ambion). Four biological replicates were hybridized to the Sentrix BeadChips Array mouse WG-6 v2 (Illumina). Data extraction was done with BeadStudio software and expression levels were normalized by a quantile method using the limma R package. The quality of the dataset was checked by using an unsupervised clustering analysis of experimental groups compared with the control. At this step, one control mouse was excluded from analyses because of pre-analytic statistical tests (Principal Variance Component Analysis) showing that some experimental issues were responsible for an external variability source. Gene ontology (GO)–based signatures were tested for their significance on our microarray data using Gene Set Enrichment Analysis (GSEA) software and statistically significant molecular signatures (false discovery rate (FDR) q.value < 0.05) were selected. Molecular signatures that were differentially modulated in VLP or $_{ncRNA}$VLP groups compared with the PBS group were mapped using Cytoscape software (23) with the "Enrichment map" plugin (24). Each dot represent a molecular signature from the Gene Ontology Database that is significantly enriched compared to the PBS group. If two of these signatures show a strong overlap between their genes, they are linked by an edge (based on the Jaccard similarity index), and the length of this edge depends on the number of genes shared by the two signatures (the more genes they share, the shorter the edge is). Signatures specifically regulated in the $_{ncRNA}$VLPs and

not shared with the VLPs were identified to characterize the specific ncRNA impact on DCs. Heatmaps were generated by using heatmap.2 R package software to show the individual gene expression in signatures of interest. Raw microarray data have been deposited in NCBI's Gene Expression Omnibus (GEO) and are accessible through GEO series accession number GSE70557 (http://www.ncbi.nlm.nih.gov/geo/query/acc.cgi?acc=GSE70557).

Quantitative PCR

Complementary DNA was generated using SuperScript VILO (Life Technologies, France) and performed reverse transcription according to the manufacturer's instructions. Quantitative PCR was performed using the 7500 Fast Real-Time PCR System (Life Technologies, France) with Fast Master Mix (Life Technologies, France) and TaqMan gene expression assay probes (Life Technologies, France). The probe IDs are Irf1: Mm01288580_m1, Irf7: Mm00516793_g1, Mx2: Mm00488995_m1, Relb: Mm00485664_m1, Rsad2: Mm00491265_m1, Slc2a6: Mm00554217_m1, Traf6: Mm00493836_m1, Xcl1: Mm00434772_m1 and 18S: Mm03928990_g1. qPCRs were performed in triplicate and the mRNA levels were normalized to that of GAPDH mRNA and 18S mRNA.

***In vitro* proliferation of antigen-specific CD8+ T cells**

Spleen cells were collected from C57BL/6, MyD88$^{-/-}$ and OT-I mice. DCs from C57Bl/6 and MyD88$^{-/-}$ mice were isolated by magnetic sorting with CD11c microbeads (Miltenyi Biotec). OT-I CD8+ T cells were isolated by negative selection using biotin-conjugated antibodies specific for CD11c, CD11b and B220 (all from BD Biosciences, Pont-de Claix, France) plus anti-biotin microbeads (Miltenyi Biotec) and stained with CFSE (Life Technologies). In a 96-well plate, 2x10^5 OT-I CFSE+ splenic cells were cultured in RPMI medium supplemented with 2 mM L-glutamine, 100 U/mL penicillin, 100 µg/mL streptomycin (all from Life Technologies, Cergy Pontoise, France) and 10% heat-inactivated fetal calf serum, with 4x10^4 CD11c+ cells (ratio 5:1) from C57Bl/6 or MyD88$^{-/-}$ mice in the presence of 5 µg of VSV-G-pseudotyped Gag-OVA VLPs or $_{ncRNA}$VLPs, or medium for control. After 3 days, proliferation and activation of OVA-specific CD8+ T cells were analyzed by flow cytometry.

***In vivo* proliferation of CD8+ or CD4+ T cells**

C57Bl/6 or MyD88$^{-/-}$ mice were immunized by i.v. injection of 1 µg of VSV-G-pseudotyped Gag-OVA VLPs or $_{ncRNA}$VLPs or PBS in the control group. 6 hours later, CFSE-stained OT-I or OT-II spleen cells containing 1.5x10^6 transgenic cells (proportion measured by flow cytometry) were i.v. injected. After 3 or 5 days, spleens were collected and proliferation of OT-I or OT-II transgenic CFSE+ cells was evaluated by flow cytometry.

Flow cytometry

Immunostaining for flow cytometry was performed with the following mAbs: V500-conjugated anti-CD4, AF700-conjugated anti-CD8, V500-conjugated anti-IA/E, biotin-conjugated anti-CD80, biotin-conjugated anti-CD44, efluor450-conjugated anti-CD86, APC-conjugated anti-Tbet, PE-conjugated anti-GATA3 (all from BD Biosciences), APC-conjugated anti-CD11c and APC-conjugated anti-Vα2 (both from eBiosciences). Biotin-conjugated antibodies were detected with PECy7-conjugated streptavidin (eBioscience). In *in vitro* assays, 7-AAD viability dye was added to exclude dead cells from the analysis. All cytometry experiments were performed with a BD^{TM} LSRII cytometer and data were analyzed using FlowJo software (Treestar).

HIV immunizations

6-week-old C57BL/6 or MyD88$^{-/-}$ female mice were immunized s.c. at weeks 0, 2 and 4 with 25 µg of HIV-gp140 pseudotyped Gag-gp33-41 VLPs or $_{ncRNA}$VLPs. At weeks 6 and 12, sera were collected from blood samples to analyze antibody responses. At week 12, mice were sacrificed to analyze cellular immune responses.

Anti-HIV humoral immune response

HIV-specific IgG antibody concentrations in the sera were evaluated by gp140-specific ELISA. Gp140 protein (kindly provided by R. Wyatt, US) was coated at 0.5 µg/mL O/N at 4°C before adding diluted sera for 2 hours at RT. Anti-mouse IgG coupled to horseradish peroxidase (HRP; Dako, Hamburg, Germany) was then added for 1 hour RT. After washing, TMB (eBioscience) was added and absorbance was read at 405 nm. 2G12 antibody (Polymun Scientific, Austria) was used as standard for determination of HIV-specific antibody concentration.

Anti-HIV cellular immune response

Spleens were collected and specific IFN-γ production by T cells was determined in a standard ELISPOT assay (Mabtech). Briefly, $5x10^5$ spleen cells were restimulated for 24 h at 37°C in 5% CO_2 with 10 µg/mL of gp33-41 peptide or 10 ng/well of gp140-pseudotyped lentiviral particles made of HIV Gag. Medium alone and concanavalin A (ConA; Sigma-Aldrich) at 3 µg/mL were used as negative and positive controls, respectively. Spots were counted with an AID ELISPOT reader (ELR03; AID, Germany). Results were expressed as spot-forming units (SFUs) per 10^6 cells.

Results

ncRNA encapsidation into VLPs

The ncRNA plasmid derived from a retroviral vector from which the coding reporter gene was deleted. Only the flanking regions (R, U5 from 5'-LTR and U3, R, U5 from 3'-LTR), the tRNA primer-binding site (PBS), the retroviral packaging signal sequence (psi) and the polypurine tract (PPT) were functional (Fig. 1A). As a result, the ncRNA plasmid produces RNA molecules that do not encode specific proteins but can be incorporated into retroviral particles by interactions between Gag and psi elements during the packaging process in addition to cellular RNAs (Fig. 1B). The presence of ncRNA was tested by RT-qPCR on pseudo-particles purified from H293T cells transfected with plasmid DNA encoding MLV-Gag, VSV-G envelope glycoproteins, and ncRNA or not. Specific detection of ncRNA was observed in pseudo-particles produced in the presence of ncRNA plasmid ($_{ncRNA}$VLPs), while the signal detected in VLPs produced in the absence of the ncRNA plasmid was equivalent to the background (Fig. 1C). Similar results were observed in pseudo-particles produced with chimeric MLV-Gag proteins fused with OVA or gp33-41 antigens (data not shown), demonstrating that ncRNA was efficiently encapsidated in the different recombinant VLPs used in this study. qPCR assay was also performed without the reverse transcription step in order to evaluate the eventual presence of contaminating ncRNA-encoding plasmid DNA in our preparations. Positive results were obtained but level of plasmid DNA was around 1000 times lower than signal observed after reverse transcription.

Wondering if the presence of the ncRNA into the particles could modify the quantity of cellular RNA packaged, we compared the total RNA quantity in $_{ncRNA}$VLP and VLP preparations and observed very similar quantities in both types of VLPs (mean of 593 ng/µg for $_{ncRNA}$VLPs, 528 ng/µg for VLPs). This suggests that the incorporation of ncRNA in VLPs does not significantly modify the total quantity of RNA carried by the particles but impact its quality since $_{ncRNA}$VLPs specifically harbor RNA of viral origin in addition to cellular RNAs. Also, to exclude the possibility that endotoxins could play a role in the VLP effect described later on, we assessed the possible LPS contamination by performing a Limulus amoebocyte lysate (LAL)-based assay on different preparations of VLPs. Results show that there are low endotoxin levels in our VLP preparations, lower actually than in a commercial OVA protein batch used as control (Fig. 1E). Importantly the endotoxin levels measured in VLPs and $_{ncRNA}$VLPs are very similar, thus guaranteeing that the comparison between the two types of VLPs is not biased by endotoxin contamination.

ncRNA carried in VLPs increases dendritic cell activation in a MyD88-dependent manner

To evaluate the ability of ncRNA to improve the immunogenicity of VLPs, we compared the capacity of VLPs and $_{ncRNA}$VLPs to activate murine DCs. C57Bl/6 immature BMDCs were cultured in the presence of 1, 5, or 10 µg of VLPs ± ncRNA for 24 hours and expression of CD80 (Fig. 2A, 2C and 2E) and CD86 (Fig. 2B, 2D and 2F) costimulation molecules were analyzed by flow cytometry. Medium alone, R848 (TLR7 ligand) and LPS (TLR4 ligand) were used as negative and two positive controls, respectively. We observed a dose-dependent activation of BMDCs with standard VLPs (in the absence of viral RNA), demonstrating their intrinsic immunogenicity and confirming our previous results observed with human DCs (10). Moreover, a significant higher expression of both CD80 and CD86 was observed with $_{ncRNA}$VLPs as compared with standard VLPs (Fig. 2E and 2F), demonstrating the adjuvant properties of encapsidated ncRNA.

Engagement of the TLR pathways was evaluated by conducting similar experiments with BMDCs from mice deficient for the myeloid differentiation primary response gene 88 (MyD88$^{-/-}$ mice), which is involved in the signaling pathways of most of the TLRs. As expected, R848 had no activation effect in MyD88$^{-/-}$ BMDCs while LPS,

which is known to induce both a MyD88-dependent and -independent pathway, still induced cell activation (Fig. 2I-J). Interestingly, very weak activation was observed with VLPs in MyD88$^{-/-}$ BMDCs and was not significantly increased with $_{ncRNA}$VLPs (Fig. 2G-L). Therefore, we first conclude that VLPs alone are able to trigger a MyD88-dependent pathway, partly explaining their immunogenicity and suggesting that VLPs are recognized by some TLRs. Secondly, as no effect of ncRNA was observed on activation of MyD88$^{-/-}$ BMDCs, this confirms that the increased activation of wild-type BMDCs is mediated by TLR activation by ncRNA, likely TLR7 and/or TLR8.

Transcriptome analysis of dendritic cells activated by VLPs or $_{ncRNA}$VLPs

In order to better characterize the intrinsic immunogenicity of MLV-derived VLPs and the mechanisms related to DC activation by ncRNA, we performed a transcriptome analysis of sorted CD11c+ cells from the spleen of C57Bl/6 mice 6 hours after intravenous injection of VLPs or $_{ncRNA}$VLPs. As expected a large set of shared genes (n = 572) was differentially expressed in both VLP or $_{ncRNA}$VLP groups. In contrast, few genes (n = 169) were specifically modulated by ncRNA. Using unsupervised analysis with multidimensional scaling, no efficient segregation between VLP and $_{ncRNA}$VLP groups were observed (not shown), confirming the high similarities between the two groups.

However, based on the differentially expressed genes and Gene Set Enrichment Analysis (GSEA), we identified signatures significantly regulated in VLP or $_{ncRNA}$VLP groups in comparison with controls. The results were mapped as a network of signatures (nodes) related by similarity (edges) in which shared signatures and specific ones of $_{ncRNA}$VLPs were indicated in gray and red, respectively (Fig. 3A). As expected, the two types of VLPs share common signaling pathways that are organized in functional modules related to immunology, including immune response, proteasome activity and viral processes (in gray). We focused on signatures that are specifically enriched in the $_{ncRNA}$VLP group, shown in red in Figure 3A. These specific signatures were related to (i) RNA transport (ii) Th1 immune response and (iii) IFN-γ/IL-4 secretion, , which is very consistent with the presence of ncRNA in VLPs and its ability to polarize the immune responses. Three of the immune-related enriched GO signatures are represented in Figure 3B, confirming the ability of ncRNA to

activate DCs and activate TLR signaling, and revealing their capacity to induce Th1-biased immune responses, as shown for example by the increased expression of Irf1 (interferon regulating factor-1) and Xcl1 genes, which are associated with Th1 responses. Notably, increased expression of eight important genes from the 3 selected signatures, including Irf1 and Xcl1, was confirmed by RT-qPCR (Fig. 3C), strengthening our results.

ncRNA increases cross-presentation of antigens carried by VLPs

We next considered the specific role of the carried ncRNA in antigen cross-presentation and CD8+ T cell activation. *In vitro* T cell proliferation experiments were performed with transgenic OT-I CD8+ T cells (specific for OVA257-264 peptide, restricted to H2-K^b MHC class I molecules) co-cultured for 3 days with wild-type or MyD88$^{-/-}$ DCs in the presence of OVA-recombinant VLPs made of Gag-OVA fusion proteins and carrying or not ncRNA. We observed that recombinant VLPs induced specific proliferation of the TCR-transgenic CD8+ T cells, which was significantly higher with $_{ncRNA}$VLPs compared with VLPs devoid of ncRNA (Fig. 4A). When the experiments were performed with MyD88$^{-/-}$ DC cells in presence of standard recombinant VLPs, we observed similar levels of proliferation to those induced by wild-type DCs, indicating that TLR recognition is not absolutely necessary for induction of CD8+ T cell proliferation (Fig. 4B). Importantly, no significant improvement of *in vitro* T cell proliferation was observed with $_{ncRNA}$VLPs in the presence of MyD88$^{-/-}$ DC cells, demonstrating that ncRNA requires MyD88-dependent signals to express its adjuvant properties.

We tested the adjuvant effect of ncRNA on *in vivo* CD8+ T cell proliferation by injecting OVA-recombinant VLPs or $_{ncRNA}$VLPs in C57BL/6 wild-type or MyD88$^{-/-}$ mice, injected 6 hours later with CFSE-stained OT-I T cells. Consistent with the *in vitro* experiments, a significantly higher proliferation of transgenic OT-I CD8+ T cells was observed at day 3 with the $_{ncRNA}$VLPs compared with VLPs (Fig. 4C and 4D), confirming the ability of ncRNA molecules to amplify CD8+ T cell responses. In contrast, no difference in CD8+ T cell proliferation was observed in MyD88$^{-/-}$ mice when VLPs and $_{ncRNA}$VLPs were compared (Fig. 4E), confirming the involvement of TLR activation in the *in vivo* adjuvant effect of ncRNA.

ncRNA improves antigen-specific CD4+ T cell activation and Th1 polarization

We also considered the specific role of the carried ncRNA in CD4+ T cell activation and differentiation. *In vivo* T cell proliferation experiments were performed with OVA-specific transgenic OT-II CD4+ T cells. Interestingly, OVA-recombinant $_{ncRNA}$VLPs significantly improved the proliferation of antigen-specific CD4+ T cells, as shown in an adoptive transfer model with OT-II cells (Fig. 4F) and compared with VLPs. The polarization of effector CD4+ T cells was investigated and intracellular staining of Tbet and GATA3 transcription factors was performed. We observed a significant increase of the ratio of the mean fluorescence intensities of T-bet and GATA3 in divided CD4+ T cells from mice immunized with $_{ncRNA}$VLPs as compared with VLPs, reflecting a Th1-biased polarization (Fig. 4G). Notably, these results were accordant with the transcriptome analysis (Fig. 3B) and confirm the ability of ncRNA to promote Th1 immune responses.

ncRNA improves vaccine specific responses in mice

Finally, we evaluated the impact of ncRNA in a vaccination model against HIV by using MLV-derived VLPs pseudotyped with HIV-1 gp140 envelope glycoproteins. The gp33-41 CD8+ T-cell specific model antigen was fused to MLV-Gag to evaluate simultaneously the cross-priming efficiency. C57Bl/6 mice were immunized subcutaneously three times every 2 weeks with HIV-pseudotyped recombinant VLPs or $_{ncRNA}$VLPs (Fig. 5A) and T cell responses were measured at week 12 by IFN-γ ELISPOT after restimulation either with gp33-41 or HIV-1 gp140 antigens. While VLPs devoid of ncRNA generated modest but significant IFN-γ T cell immune responses against gp33-41, $_{ncRNA}$VLPs significantly increased the responses (Fig. 5B). Adding ncRNA also significantly increased the gp140-specific IFN-γ T cell immune responses (Fig. 5C), highlighting the adjuvant properties of ncRNA in inducing HIV-specific Th1 immune responses in a vaccine approach. Importantly, the improvement of CD4+ T cell immune responses by ncRNA was TLR-mediated since no significant differences were observed between VLPs and $_{ncRNA}$VLPs when experiments were conducted in MyD88$^{-/-}$ mice (Fig. 5B-C).

Antibody responses were evaluated by measuring the anti-gp140 specific antibody concentration in the serum of vaccinated mice, either at week 6 (Fig. 5D) or at week 12 (Fig. 5E) to assess its long-term persistence. At the early time point after immunizations, high antibody concentrations were detected but no difference was

observed between the two groups (Fig. 5D). In contrast, at week 12, anti-gp140 antibody concentration had dramatically dropped in the group immunized with VLPs, while mice immunized with $_{ncRNA}$VLPs still presented high levels of anti-gp140 antibodies (Fig 5E), revealing a capacity of the ncRNA adjuvant to maintain HIV-specific antibody levels in the sera of immunized mice.

Discussion

VLPs are considered as highly immunogenic vaccines and are used as an antigenic platform to increase the immunogenicity of antigens (2). Here, we studied the immunogenic properties of MLV-derived VLPs and propose an adjuvant strategy to increase their immunogenicity. We confirmed the ability of these VLPs to induce activation of antigen-presenting cells. Indeed, efficient uptake of VLPs and activation of murine BMDCs were demonstrated, which represent the prerequisite for the high immunological activity of recombinant VLPs and confirm our previous observations with human monocyte–derived DCs (10). DC activation was confirmed with VLPs highly purified by anion exchange chromatography on Q Sepharose (data not shown), demonstrating that their immunogenicity is not due to the presence of contaminants in the VLP preparation, which was already reported in baculovirus-expressed VLPs and may partially explain the enhanced immunogenicity of these types of VLPs (25). By contrast, it is well known that in the human cell lines production systems, human surface proteins are incorporated in the membrane of VLPs, and these proteins probably play a role in the observed immunogenicity of particles, as it has been shown for tetraspanins for example (26). Moreover, we demonstrated that MLV VLPs induce efficient cross-presentation as shown by *in vitro* and *in vivo* proliferation of CD8+ T cells against displayed antigens. Consistent with our findings, other groups previously demonstrated that antigens carried by different VLPs, including HBs- and HCV-derived VLPs, can be efficiently cross-presented by DCs (27),(28).

Several mechanisms could explain the intrinsic adjuvant-like properties of MLV VLPs. Based on transcriptome analyses, we observed that MLV VLPs positively regulate numerous immunological signatures related to the immune response, proteasome activity and viral processes (Fig. 3A). Interestingly, experiments conducted with

458 MyD88$^{-/-}$ DCs revealed that the Toll-like receptor pathways are also involved in VLP
459 immunogenicity (Fig. 2). We observed a significant increase of MyD88 and TLR2
460 gene expression in DC transcriptome studies that was confirmed by TLR2 activation
461 using the Invivogen TLR screening® assay (data not shown). However, even if TLR
462 seems to be involved in VLP-induced DC activation, MyD88 signaling is not sufficient
463 to fully explain the immune properties of MLV VLPs, since T-cell immune responses
464 observed in MyD88$^{-/-}$ and wild-type mice after OVA-recombinant VLP immunization
465 were equal (Fig. 4). Other mechanisms could be linked to the high immunogenicity of
466 MLV VLPs. Notably, disruption of the structure of VLPs by boiling them for 10
467 minutes led to a dramatic loss of DC activation (data not shown), demonstrating that
468 the particular nature of VLPs confers them intrinsic adjuvant properties. However, we
469 assume that VLPs immunogenicity may be overestimated since VLPs were prepared
470 in human 293T cells and tested in mice.

471 Otherwise, we describe in this study a novel adjuvant strategy for vaccination with
472 MLV VLPs using ncRNA, a non-coding single-stranded RNA molecule capable of
473 being packaged in the particles. As it is well known that numerous host cell RNAs
474 can be encapsulated in MLV particles (29)(30), we postulated that ncRNA can be
475 enriched in VLPs due to the presence of the *psi* sequence, and can express adjuvant
476 properties after binding to TLR7 and/or TLR8. TLR7/8 ligands have already shown
477 great results as immunomodulating therapeutic agents (31)'(32) and are very
478 promising vaccine adjuvants, including against HIV (33)'(34). Consistently with these
479 results, TLR7/8 agonists have been shown to efficiently activate and induce cytokine
480 secretion by DCs, in a MyD88-dependent way (35)'(36)'(37). Here, we demonstrated *in*
481 *vitro* and *in vivo* that ncRNA improves VLP immunogenicity after TLR recognition.
482 Transcriptome analyses reveal that ncRNA-induced DC maturation is linked to the
483 NF-κB signaling pathway, as shown by the increased expression of Traf6, Batf,
484 Batf2, RelB in murine DCs, and a significant modulation of the TLR signaling related
485 genes (Fig. 3B-C). Among those genes, Rsad2 (or Viperin) which has already been
486 shown to promote interferon-β secretion in response to TLR7 ligand (38) and acts on
487 antigen presentation (39) as shown by ubiquitin D (Ubd) gene upregulation in splenic
488 DCs was up-regulated. We also observed a significant increase in numerous genes
489 involved in the response to interferons such as Mx2, Oas1, Oas2, Socs3, Irf7 and
490 several other interferon-inducible genes, suggesting that ncRNA triggers interferon

secretion. Interestingly, these genes have also been reported by Pulandran et al. to play a key role in vaccine responses against commercialized vaccines and may be predictive for an efficient vaccine response (40–43).

TLR7/8 ligands have been especially used for their capacity to enhance CD8+ T cell responses against numerous antigens (33),(44),(45),(46). Similarly, we show here that ncRNA had a positive effect on CD8+ T cell proliferation *in vitro* and *in vivo* in an OVA model (Fig. 4) and was confirmed with the gp33-41 antigen model (Fig. 5). Improvement of antigen cross-presentation by ncRNA could be explained by modulation of antigen processing (16),(47),(48),(49). However, further experiments are required to evaluate if enhanced co-stimulatory molecule expression and/or secreted cytokine induced by ncRNA could alternatively explain the improvement of CD8+ T cell activation.

ncRNA also modulates CD4+ T cell polarization. Indeed, we observed that ncRNA promotes Th1 CD4+ responses rather than Th2 CD4+ responses, as (i) secretion by BMDCs of TNFα is significantly increased, but not of IL-4, (ii) T-bet transcription factor expression is slightly increased *in vivo* in activated CD4+ T cells while GATA3 expression is slightly decreased, and (iii) transcriptome studies revealed Th1 response-associated signatures. More specifically, upregulation of the Irf1 gene, which is involved in the regulation of interferon secretion and DC maturation associated with Th1 polarization (50), was observed and confirmed by RT-qPCR. We also showed in the presence of ncRNA a higher expression of the Xcl1 gene, which has been shown to be involved in antigen cross-presentation by DCs (51), and upregulation of the Slc2a6 gene that correlates with the magnitude of the antigen-specific CD8+ T cell responses (52). These observations are therefore consistent with the ability of ncRNA to improve CD8+ T cell proliferation and supported by others demonstrating the role of TLR7/8 ligands in inducing Th1 responses (53),(54). Altogether, we think ncRNA could be particularly favorable for HIV vaccine development, since a Th2-biased CD4+ T cell response has been associated with disease progression (54),(55), while Th1 responses have been shown to favor anti-HIV-1 immunity (56). In the vaccination experiments, we observed that $_{ncRNA}$VLPs induce longer lasting humoral responses. We believe $_{ncRNA}$VLPs are able to activate more efficiently follicular helper T cells, leading to a better memory induction, as it

523 has already been shown with a TLR3 ligand encapsidated in HIV-derived VLPs (57).
524 This question is currently under investigation in our laboratory.

525 While VLPs and $_{ncRNA}$VLPs have similar levels of total packaged RNA, we
526 demonstrated here that ncRNA carried into $_{ncRNA}$VLPs has a unique TLR-dependent
527 adjuvant property in contrast to host RNAs. One remaining question concerns the
528 molecular pattern that confers its immunogenicity to ncRNA. Specific TLR7/8 ligand
529 motifs such as polyuridine sequences that would explain the induced MyD88-
530 signaling were not identified in the ncRNA sequence. Additional efforts should be
531 made in the near future to better characterize ncRNA-related immunogenicity and
532 establish a TLR7/8-dependent mechanism.

533 In conclusion, this study provides new evidence of MLV-derived VLP
534 immunogenicity, and demonstrates the advantages of using ncRNA as an
535 encapsulated adjuvant molecule. These observations warrant further evaluation in
536 prime-boost and/or in mucosal vaccine approaches, especially for HIV vaccination,
537 but also in allergen-specific immunotherapy with the specific aim of shifting the
538 immune response from the allergic Th2 to the non-allergic Th1 responses.

539

540 **Acknowledgments**

541 This work was supported by ANRS, UPMC and INSERM.

542 We thank the personnel of the Post-Genomic Platform (P3S) of the Pitié-Salpêtrière
543 Hospital in Paris for their involvement in the transcriptome experiments, and Omar
544 Chuquisana and Faustine Brimaud for their technical help.

545

References

1. Kushnir N, Streatfield SJ, Yusibov V. 2012. Virus-like particles as a highly efficient vaccine platform: diversity of targets and production systems and advances in clinical development. Vaccine 31:58–83.

2. Bachmann MF, Jennings GT. 2010. Vaccine delivery: a matter of size, geometry, kinetics and molecular patterns. Nat Rev Immunol 10:787–796.

3. Noad R, Roy P. 2003. Virus-like particles as immunogens. Trends Microbiol 11:438–444.

4. Chackerian B. 2007. Virus-like particles: flexible platforms for vaccine development. Expert Rev Vaccines 6:381–390.

5. Campo JJ, Sacarlal J, Aponte JJ, Aide P, Nhabomba AJ, Dobaño C, Alonso PL. 2014. Duration of vaccine efficacy against malaria: 5th year of follow-up in children vaccinated with RTS,S/AS02 in Mozambique. Vaccine 32:2209–2216.

6. Garrone P, Fluckiger A-C, Mangeot PE, Gauthier E, Dupeyrot-Lacas P, Mancip J, Cangialosi A, Du Chéné I, LeGrand R, Mangeot I, Lavillette D, Bellier B, Cosset F-L, Tangy F, Klatzmann D, Dalba C. 2011. A prime-boost strategy using virus-like particles pseudotyped for HCV proteins triggers broadly neutralizing antibodies in macaques. Sci Transl Med 3:94ra71.

7. Bellier B, Dalba C, Clerc B, Desjardins D, Drury R, Cosset F-L, Collins M, Klatzmann D. 2006. DNA vaccines encoding retrovirus-based virus-like particles induce efficient immune responses without adjuvant. Vaccine 24:2643–2655.

8. Bellier B, Huret C, Miyalou M, Desjardins D, Frenkiel M-P, Despres P, Tangy F, Dalba C, Klatzmann D. 2009. DNA vaccines expressing retrovirus-like particles are efficient immunogens to induce neutralizing antibodies. Vaccine 27:5772–5780.

570 9. Huret C, Desjardins D, Miyalou M, Levacher B, Amadoudji Zin M, Bonduelle O,
571 Combadière B, Dalba C, Klatzmann D, Bellier B. 2013. Recombinant retrovirus-derived
572 virus-like particle-based vaccines induce hepatitis C virus-specific cellular and
573 neutralizing immune responses in mice. Vaccine 31:1540–1547.

574 10. Lescaille G, Pitoiset F, Macedo R, Baillou C, Huret C, Klatzmann D, Tartour E, Lemoine
575 FM, Bellier B. 2013. Efficacy of DNA vaccines forming e7 recombinant retroviral virus-
576 like particles for the treatment of human papillomavirus-induced cancers. Hum Gene
577 Ther 24:533–544.

578 11. Sindhu S, Toma E, Cordeiro P, Ahmad R, Morisset R, Menezes J. 2006. Relationship of
579 in vivo and ex vivo levels of TH1 and TH2 cytokines with viremia in HAART patients
580 with and without opportunistic infections. J Med Virol 78:431–439.

581 12. García-Díaz D, Rodríguez I, Santisteban Y, Márquez G, Terrero Y, Brown E, Iglesias E.
582 2013. Th2-Th1 shift with the multiantigenic formulation TERAVAC-HIV-1 in Balb/c mice.
583 Immunol Lett 149:77–84.

584 13. Olive C. 2012. Pattern recognition receptors: sentinels in innate immunity and targets of
585 new vaccine adjuvants. Expert Rev Vaccines 11:237–256.

586 14. Steinhagen F, Kinjo T, Bode C, Klinman DM. 2011. TLR-based immune adjuvants.
587 Vaccine 29:3341–3355.

588 15. Beutler BA. 2009. TLRs and innate immunity. Blood 113:1399–1407.

589 16. Crespo MI, Zacca ER, Núñez NG, Ranocchia RP, Maccioni M, Maletto BA, Pistoresi-
590 Palencia MC, Morón G. 2013. TLR7 Triggering with Polyuridylic Acid Promotes Cross-
591 Presentation in CD8α+ Conventional Dendritic Cells by Enhancing Antigen Preservation
592 and MHC Class I Antigen Permanence on the Dendritic Cell Surface. J Immunol
593 190:948–960.

17. Fehres CM, Bruijns SCM, van Beelen AJ, Kalay H, Ambrosini M, Hooijberg E, Unger WWJ, de Gruijl TD, van Kooyk Y. 2014. Topical rather than intradermal application of the TLR7 ligand imiquimod leads to human dermal dendritic cell maturation and CD8(+) T-cell cross-priming. Eur J Immunol.

18. Shirota H, Klinman DM. 2014. TLR-9 agonist immunostimulatory sequence adjuvants linked to cancer antigens. Methods Mol Biol Clifton NJ 1139:337–344.

19. Soong R-S, Song L, Trieu J, Knoff J, He L, Tsai YC, Huh W, Chang Y-N, Cheng W-F, Roden RBS, Wu T-C, Hung C-F. 2014. Toll like receptor agonist imiquimod facilitates antigen-specific CD8+ T cell accumulation in the genital tract leading to tumor control through interferon-γ. Clin Cancer Res clincanres.0344.2014.

20. Vasilakos JP, Tomai MA. 2013. The use of Toll-like receptor 7/8 agonists as vaccine adjuvants. Expert Rev Vaccines 12:809–819.

21. Adachi O, Kawai T, Takeda K, Matsumoto M, Tsutsui H, Sakagami M, Nakanishi K, Akira S. 1998. Targeted disruption of the MyD88 gene results in loss of IL-1- and IL-18-mediated function. Immunity 9:143–150.

22. Yee JK, Friedmann T, Burns JC. 1994. Generation of high-titer pseudotyped retroviral vectors with very broad host range. Methods Cell Biol 43 Pt A:99–112.

23. Shannon P, Markiel A, Ozier O, Baliga NS, Wang JT, Ramage D, Amin N, Schwikowski B, Ideker T. 2003. Cytoscape: a software environment for integrated models of biomolecular interaction networks. Genome Res 13:2498–2504.

24. Merico D, Isserlin R, Bader GD. 2011. Visualizing gene-set enrichment results using the Cytoscape plug-in enrichment map. Methods Mol Biol Clifton NJ 781:257–277.

25. Margine I, Martinez-Gil L, Chou Y-Y, Krammer F. 2012. Residual baculovirus in insect cell-derived influenza virus-like particle preparations enhances immunogenicity. PloS One 7:e51559.

26. Soares HR, Castro R, Tomás HA, Rodrigues AF, Gomes-Alves P, Bellier B, Klatzmann D, Carrondo MJT, Alves PM, Coroadinha AS. 2016. Tetraspanins displayed in retrovirus-derived virus-like particles and their immunogenicity. Vaccine 34:1634–1641.

27. Moffat JM, Cheong W-S, Villadangos JA, Mintern JD, Netter HJ. 2013. Hepatitis B virus-like particles access major histocompatibility class I and II antigen presentation pathways in primary dendritic cells. Vaccine 31:2310–2316.

28. Barth H, Ulsenheimer A, Pape GR, Diepolder HM, Hoffmann M, Neumann-Haefelin C, Thimme R, Henneke P, Klein R, Paranhos-Baccalà G, Depla E, Liang TJ, Blum HE, Baumert TF. 2005. Uptake and presentation of hepatitis C virus-like particles by human dendritic cells. Blood 105:3605–3614.

29. Onafuwa-Nuga AA, King SR, Telesnitsky A. 2005. Nonrandom packaging of host RNAs in moloney murine leukemia virus. J Virol 79:13528–13537.

30. Rulli SJ, Hibbert CS, Mirro J, Pederson T, Biswal S, Rein A. 2007. Selective and nonselective packaging of cellular RNAs in retrovirus particles. J Virol 81:6623–6631.

31. Fife KH, Meng T-C, Ferris DG, Liu P. 2008. Effect of Resiquimod 0.01% Gel on Lesion Healing and Viral Shedding When Applied to Genital Herpes Lesions. Antimicrob Agents Chemother 52:477–482.

32. Wu CCN, Hayashi T, Takabayashi K, Sabet M, Smee DF, Guiney DD, Cottam HB, Carson DA. 2007. Immunotherapeutic activity of a conjugate of a Toll-like receptor 7 ligand. Proc Natl Acad Sci U S A 104:3990–3995.

639 33. Wille-Reece U, Flynn BJ, Loré K, Koup RA, Kedl RM, Mattapallil JJ, Weiss WR,
640 Roederer M, Seder RA. 2005. HIV Gag protein conjugated to a Toll-like receptor 7/8
641 agonist improves the magnitude and quality of Th1 and CD8+ T cell responses in
642 nonhuman primates. Proc Natl Acad Sci U S A 102:15190–15194.

643 34. Moody MA, Santra S, Vandergrift NA, Sutherland LL, Gurley TC, Drinker MS, Allen AA,
644 Xia S-M, Meyerhoff RR, Parks R, Lloyd KE, Easterhoff D, Alam SM, Liao H-X, Ward
645 BM, Ferrari G, Montefiori DC, Tomaras GD, Seder RA, Letvin NL, Haynes BF. 2014.
646 Toll-like receptor 7/8 (TLR7/8) and TLR9 agonists cooperate to enhance HIV-1
647 envelope antibody responses in rhesus macaques. J Virol 88:3329–3339.

648 35. Gibson SJ, Lindh JM, Riter TR, Gleason RM, Rogers LM, Fuller AE, Oesterich JL,
649 Gorden KB, Qiu X, McKane SW, Noelle RJ, Miller RL, Kedl RM, Fitzgerald-Bocarsly P,
650 Tomai MA, Vasilakos JP. 2002. Plasmacytoid dendritic cells produce cytokines and
651 mature in response to the TLR7 agonists, imiquimod and resiquimod. Cell Immunol
652 218:74–86.

653 36. Ahonen CL, Gibson SJ, Smith RM, Pederson LK, Lindh JM, Tomai MA, Vasilakos JP.
654 1999. Dendritic cell maturation and subsequent enhanced T-cell stimulation induced
655 with the novel synthetic immune response modifier R-848. Cell Immunol 197:62–72.

656 37. Hemmi H, Kaisho T, Takeuchi O, Sato S, Sanjo H, Hoshino K, Horiuchi T, Tomizawa H,
657 Takeda K, Akira S. 2002. Small anti-viral compounds activate immune cells via the
658 TLR7 MyD88-dependent signaling pathway. Nat Immunol 3:196–200.

659 38. Saitoh T, Satoh T, Yamamoto N, Uematsu S, Takeuchi O, Kawai T, Akira S. 2011.
660 Antiviral protein Viperin promotes Toll-like receptor 7- and Toll-like receptor 9-mediated
661 type I interferon production in plasmacytoid dendritic cells. Immunity 34:352–363.

662 39. Lombardi V, Van Overtvelt L, Horiot S, Moingeon P. 2009. Human dendritic cells
663 stimulated via TLR7 and/or TLR8 induce the sequential production of Il-10, IFN-gamma,
664 and IL-17A by naive CD4+ T cells. J Immunol Baltim Md 1950 182:3372–3379.

665 40. Querec TD, Akondy RS, Lee EK, Cao W, Nakaya HI, Teuwen D, Pirani A, Gernert K,
666 Deng J, Marzolf B, Kennedy K, Wu H, Bennouna S, Oluoch H, Miller J, Vencio RZ,
667 Mulligan M, Aderem A, Ahmed R, Pulendran B. 2009. Systems biology approach
668 predicts immunogenicity of the yellow fever vaccine in humans. Nat Immunol 10:116–
669 125.

670 41. Gaucher D, Therrien R, Kettaf N, Angermann BR, Boucher G, Filali-Mouhim A, Moser
671 JM, Mehta RS, Drake DR, Castro E, Akondy R, Rinfret A, Yassine-Diab B, Said EA,
672 Chouikh Y, Cameron MJ, Clum R, Kelvin D, Somogyi R, Greller LD, Balderas RS,
673 Wilkinson P, Pantaleo G, Tartaglia J, Haddad EK, Sékaly R-P. 2008. Yellow fever
674 vaccine induces integrated multilineage and polyfunctional immune responses. J Exp
675 Med 205:3119–3131.

676 42. Nakaya HI, Wrammert J, Lee EK, Racioppi L, Marie-Kunze S, Haining WN, Means AR,
677 Kasturi SP, Khan N, Li G-M, McCausland M, Kanchan V, Kokko KE, Li S, Elbein R,
678 Mehta AK, Aderem A, Subbarao K, Ahmed R, Pulendran B. 2011. Systems biology of
679 vaccination for seasonal influenza in humans. Nat Immunol 12:786–795.

680 43. Li S, Rouphael N, Duraisingham S, Romero-Steiner S, Presnell S, Davis C, Schmidt
681 DS, Johnson SE, Milton A, Rajam G, Kasturi S, Carlone GM, Quinn C, Chaussabel D,
682 Palucka AK, Mulligan MJ, Ahmed R, Stephens DS, Nakaya HI, Pulendran B. 2014.
683 Molecular signatures of antibody responses derived from a systems biology study of
684 five human vaccines. Nat Immunol 15:195–204.

685 44. Wysocka M, Newton S, Benoit BM, Introcaso C, Hancock AS, Chehimi J, Richardson
686 SK, Gelfand JM, Montaner LJ, Rook AH. 2007. Synthetic imidazoquinolines potently

687 and broadly activate the cellular immune response of patients with cutaneous T-cell
688 lymphoma: synergy with interferon-gamma enhances production of interleukin-12. Clin
689 Lymphoma Myeloma 7:524–534.

690 45. Lebel M-È, Daudelin J-F, Chartrand K, Tarrab E, Kalinke U, Savard P, Labrecque N,
691 Leclerc D, Lamarre A. 2014. Nanoparticle adjuvant sensing by TLR7 enhances CD8+ T
692 cell-mediated protection from Listeria monocytogenes infection. J Immunol Baltim Md
693 1950 192:1071–1078.

694 46. Wille-Reece U, Wu C, Flynn BJ, Kedl RM, Seder RA. 2005. Immunization with HIV-1
695 Gag Protein Conjugated to a TLR7/8 Agonist Results in the Generation of HIV-1 Gag-
696 Specific Th1 and CD8+ T Cell Responses. J Immunol 174:7676–7683.

697 47. Oh JZ, Kurche JS, Burchill MA, Kedl RM. 2011. TLR7 enables cross-presentation by
698 multiple dendritic cell subsets through a type I IFN-dependent pathway. Blood
699 118:3028–3038.

700 48. Stephenson RM, Lim CM, Matthews M, Dietsch G, Hershberg R, Ferris RL. 2013. TLR8
701 stimulation enhances cetuximab-mediated natural killer cell lysis of head and neck
702 cancer cells and dendritic cell cross-priming of EGFR-specific CD8+ T cells. Cancer
703 Immunol Immunother CII 62:1347–1357.

704 49. Oh JZ, Kedl RM. 2010. The capacity to induce cross-presentation dictates the success
705 of a TLR7 agonist-conjugate vaccine for eliciting cellular immunity. J Immunol Baltim Md
706 1950 185:4602–4608.

707 50. Castaldello A, Sgarbanti M, Marsili G, Brocca-Cofano E, Remoli AL, Caputo A, Battistini
708 A. 2010. Interferon regulatory factor-1 acts as a powerful adjuvant in tat DNA based
709 vaccination. J Cell Physiol 224:702–709.

710 51. Kroczek RA, Henn V. 2012. The Role of XCR1 and its Ligand XCL1 in Antigen Cross-
711 Presentation by Murine and Human Dendritic Cells. Front Immunol 3:14.

712 52. Buonaguro L, Wang E, Tornesello ML, Buonaguro FM, Marincola FM. 2011. Systems
713 biology applied to vaccine and immunotherapy development. BMC Syst Biol 5:146.

714 53. Wagner TL, Ahonen CL, Couture AM, Gibson SJ, Miller RL, Smith RM, Reiter MJ,
715 Vasilakos JP, Tomai MA. 1999. Modulation of TH1 and TH2 cytokine production with
716 the immune response modifiers, R-848 and imiquimod. Cell Immunol 191:10–19.

717 54. Chang BA, Cross JL, Najar HM, Dutz JP. 2009. Topical resiquimod promotes priming of
718 CTL to parenteral antigens. Vaccine 27:5791–5799.

719 55. Wang J, Harada A, Matsushita S, Matsumi S, Zhang Y, Shioda T, Nagai Y, Matsushima
720 K. 1998. IL-4 and a glucocorticoid up-regulate CXCR4 expression on human CD4+ T
721 lymphocytes and enhance HIV-1 replication. J Leukoc Biol 64:642–649.

722 56. Pleguezuelos O, Stoloff GA, Caparrós-Wanderley W. 2013. Synthetic immunotherapy
723 induces HIV virus specific Th1 cytotoxic response and death of an HIV-1 infected
724 human cell line through classic complement activation. Virol J 10:107.

725 57. Poteet E, Lewis P, Chen C, Ho SO, Do T, Chiang S, Labranche C, Montefiori D, Fujii G,
726 Yao Q. 2016. Toll-like receptor 3 adjuvant in combination with virus-like particles elicit a
727 humoral response against HIV. Vaccine 34:5886–5894.

728

Figure legends

Figure 1

ncRNA system and validation of $_{ncRNA}$VLPs. (A) Structure of the ncRNA encoding plasmid. Box sizes indicates the relative length of the genetic sequences according to the scale provided. CMV: cytomegalovirus immediate-early promoter; psi: retroviral encapsidation sequence; U3, R, U5: MLV-long terminal repeat (LTR) sequences. **(B)** Schematic representation of MLV-derived standard VLPs (left) and $_{ncRNA}$VLPs (right). Packaged cellular RNAs and ncRNA (two copies of single-stranded virus-derived RNA) are illustrated. **(C)** Validation by RT-qPCR of the presence of ncRNA in the pseudo-particles. Gray curves: VLPs; black curves: $_{ncRNA}$VLPs. Untransfected cell lysate was used as negative control (dashed curves). Duplicates of one experiment representative of three are shown. **(D)** ncRNA-specific qPCR conducted on VLPs or $_{ncRNA}$VLPs, with (plain curves) or without (dashed curves) reverse transcriptase step. **(E)** Evaluation of endotoxin levels in three different production batches of VLPs and $_{ncRNA}$VLPs using LAL assay. Commercial OVA protein batch was used as control.

Figure 2

***In vitro* effect of VLPs carrying or not ncRNA on bone marrow–derived dendritic cell activation.** Immature BMDCs from C57BL/6 **(A-F)** or MyD88$^{-/-}$ **(G-L)** mice were incubated for 24 hours in the presence of 1, 5 or 10 µg/mL of VSV-G pseudotyped MLV-Gag VLPs or $_{ncRNA}$VLPs. CD80 and CD86 expressions were analyzed by flow cytometry. Representative histograms of CD80 **(A, G)** and CD86 **(B, H)** on C57BL/6 BMDCs **(A-B)** or MyD88$^{-/-}$ BMDCs **(G-H)** cultured with 5 µg/mL of VLPs (thin line), $_{ncRNA}$VLPs (thick line) or medium alone (plain histogram) are shown. Related percentages of CD80+ **(C, I)** and CD86+ **(D, J)** were represented. Medium alone, LPS (100 ng/mL) and R848 (1 µg/mL) were used as negative control and two positive controls, respectively. Results represent the mean + SD of duplicates for each dose of VLPs from one experiment representative of two (**C-D, I-J**) and the means +/- SEM of two independent experiments with the dose of 5 µg/mL are represented for CD80 **(E, K)** and CD86 **(F, L)** for C57BL/6 **(E, F)** and MyD88$^{-/-}$ **(K, L)** BMDCs. * $p \leq 0.05$, ns: not significant; Mann-Whitney test.

Figure 3

Transcriptome analysis of splenic dendritic cells after *in vivo* injection of VLPs or $_{ncRNA}$VLPs. Dendritic-specific gene set enrichment analysis using Gene Ontology database signatures allowed us to identify molecular signatures that are differentially enriched in VLP and $_{ncRNA}$VLP groups compared with PBS. **(A)** Results were mapped using Cytoscape software as a network of signatures (nodes) related by similarity (edges). Node size is proportional to the total number of genes in each set. Groups of functionally related signatures are circled and labeled (modules). Grey nodes represent signatures shared between VLP and $_{ncRNA}$VLP groups; red nodes represent signatures that are specific for the $_{ncRNA}$VLP group. FDR q-value = 0.05, P-value = 0.005. **(B)** Heatmap showing three ncRNA-specific signatures. Samples were clustered using a distance-based hierarchical clustering regarding the gene expression. The heatmap colors represent the gene expression (red for high, black for middle, and green for low expression). The Gene Ontology exact names of signatures are “Dendritic cell differentiation” for DC differentiation, “Positive regulation of Toll-Like receptor signaling pathways” for TLR signaling, and “Positive regulation of T helper type 1 immune response” for Th1 response. **(C)** Validation by RT-qPCR of the relative quantity of eight different genes from the three selected signatures.

Figure 4

***In vitro* and *in vivo* effects of VLPs carrying or not ncRNA on T cell proliferation and polarization. (A, B)** *In vitro* proliferation of antigen-specific CD8+ T cells. CFSE-stained OVA-specific OT-I splenic lymphocytes were cultured for 3 days with antigen-presenting cells from C57BL/6 **(A)** or MyD88$^{-/-}$ **(B)** in the presence of 5 µg/mL of VSV-G pseudotyped Gag-OVA VLPs (gray bars) or $_{ncRNA}$VLPs (black bars). Percentages of divided cells were evaluated by flow cytometry analysis of CFSE-low cells among CD8+ Vα2+ live cells. Medium alone and OVA-I peptide were used as negative and positive controls, respectively. Means of triplicates from three independent experiments are shown. **(C-E)** *In vivo* proliferation of antigen-specific CD8+ T cells. C57BL/6 or MyD88$^{-/-}$ mice (n = 5 per group) were injected i.v. with 1 µg of VSV-G pseudotyped Gag-OVA VLPs or $_{ncRNA}$VLPs, and PBS in the control group. Six hours later mice received 1.5x10^{6} CFSE+ OVA-specific CD8+ T cells from OT-I mice. After 3 days, spleens were collected and proliferation of OVA-specific CD8+ T cells was evaluated by flow cytometry. One representative dot plot of the CFSE profile from

each group is depicted in **(C)**. Percentages of divided OVA-specific CD8+ T cells for each dose in C57BL/6 **(D)** and MyD88$^{-/-}$ mice **(E)** are shown. Results represent the mean values +SEM. **(F, G)** *In vivo* proliferation and differentiation of antigen-specific CD4+ T cells. The same experiment as in (**D**) was conducted with OT-II cells instead of OT-I cells. **(F)** Means of the percentage of divided OVA-specific CD4+ T cells and SEM are shown. Geometric means (MFI) ratios of Tbet : GATA3 expression among divided CD4+ T cells are represented in **(G)**. * $p \leq 0.05$, ** $p \leq 0.01$, ns: not significant; Mann-Whitney test.

Figure 5:

T- and B-cell immune responses in mice vaccinated with HIV-pseudotyped VLPs carrying or not ncRNA. (A) Schematic representation of the vaccination protocol. C57BL/6 or MyD88-/- mice (n = 5 per group) were immunized 3 times at two-week intervals with 25 µg of HIV-pseudotyped Gag-gp33-41 VLPs or $_{ncRNA}$VLPs. Sera were collected from blood samples at weeks 6 and 12. **(B, C)** Cellular responses were evaluated at week 12 by standard IFN-γ ELISPOT after specific restimulation with either gp33-41 (B) or HIV-gp140 (**C**). Results represent individual values and group means expressed as number of spot forming units (SFUs) per million of splenocytes. **(D, E)** Specific anti-gp140 antibody concentrations were evaluated in serum of immunized or naïve C57BL/6 mice by anti-GP120 ELISA at weeks 6 (**D**) and 12 (**E**). Results represent the mean values + SEM of measured concentrations. * $p \leq 0.05$, ** $p \leq 0.01$; Mann-Whitney test.

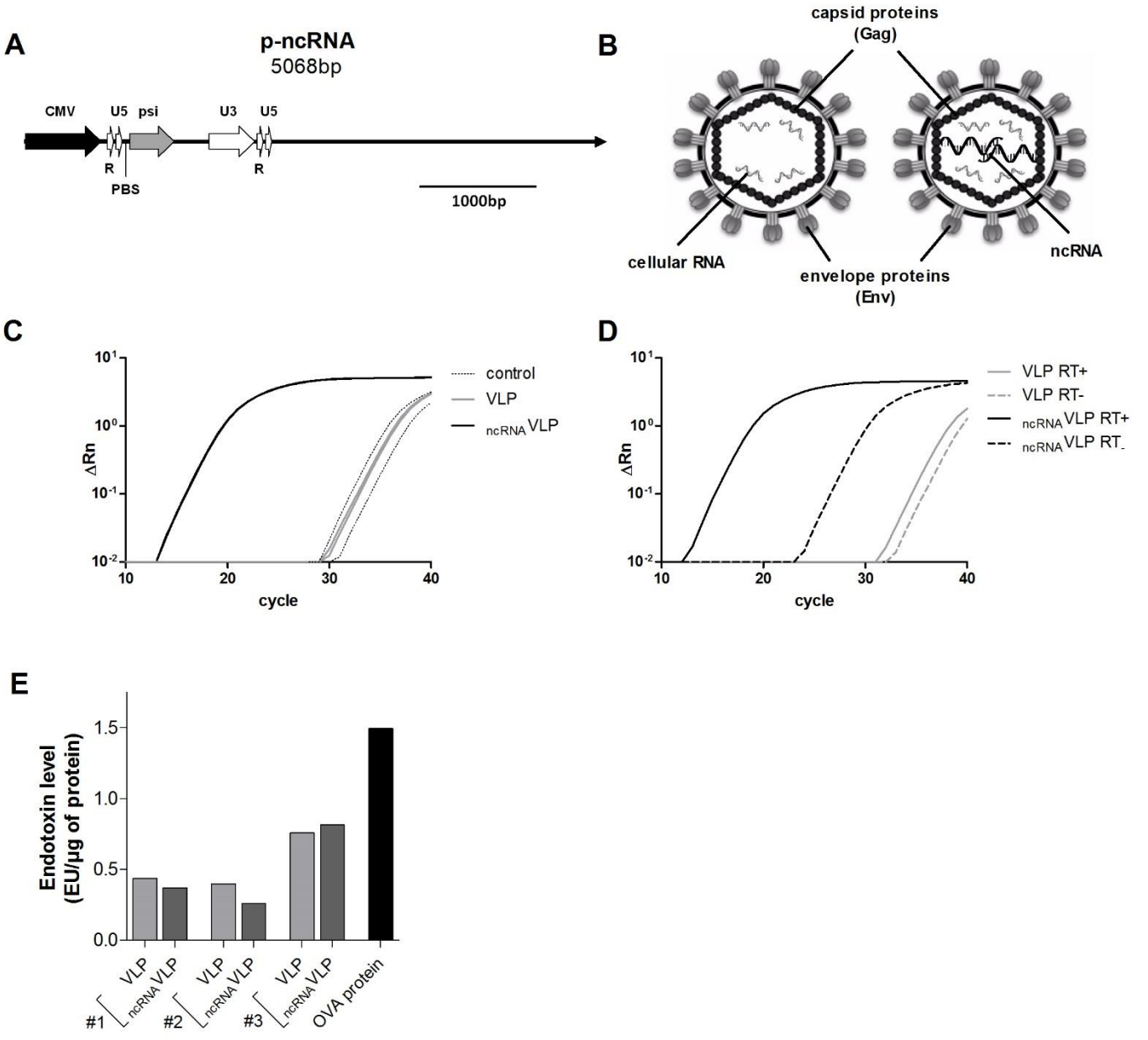

Figure 1:

ncRNA system and validation of $_{ncRNA}$VLPs. (A) Structure of the ncRNA encoding plasmid. Box sizes indicates the relative length of the genetic sequences according to the scale provided. CMV: cytomegalovirus immediate-early promoter; psi: retroviral encapsidation sequence; U3, R, U5: MLV-long terminal repeat (LTR) sequences. **(B)** Schematic representation of MLV-derived standard VLPs (left) and $_{ncRNA}$VLPs (right). Packaged cellular RNAs and ncRNA (two copies of single-stranded virus-derived RNA) are illustrated. **(C)** Validation by RT-qPCR of the presence of ncRNA in the pseudo-particles. Gray curves: VLPs; black curves: $_{ncRNA}$VLPs. Untransfected cell lysate was used as negative control (dashed curves). Duplicates of one experiment representative of three are shown. **(D)** ncRNA-specific qPCR conducted on VLPs or $_{ncRNA}$VLPs, with (plain curves) or without (dashed curves) reverse transcriptase step. **(E)** Evaluation of endotoxin levels in three different production batches of VLPs and $_{ncRNA}$VLPs using LAL assay. Commercial OVA protein batch was used as control.

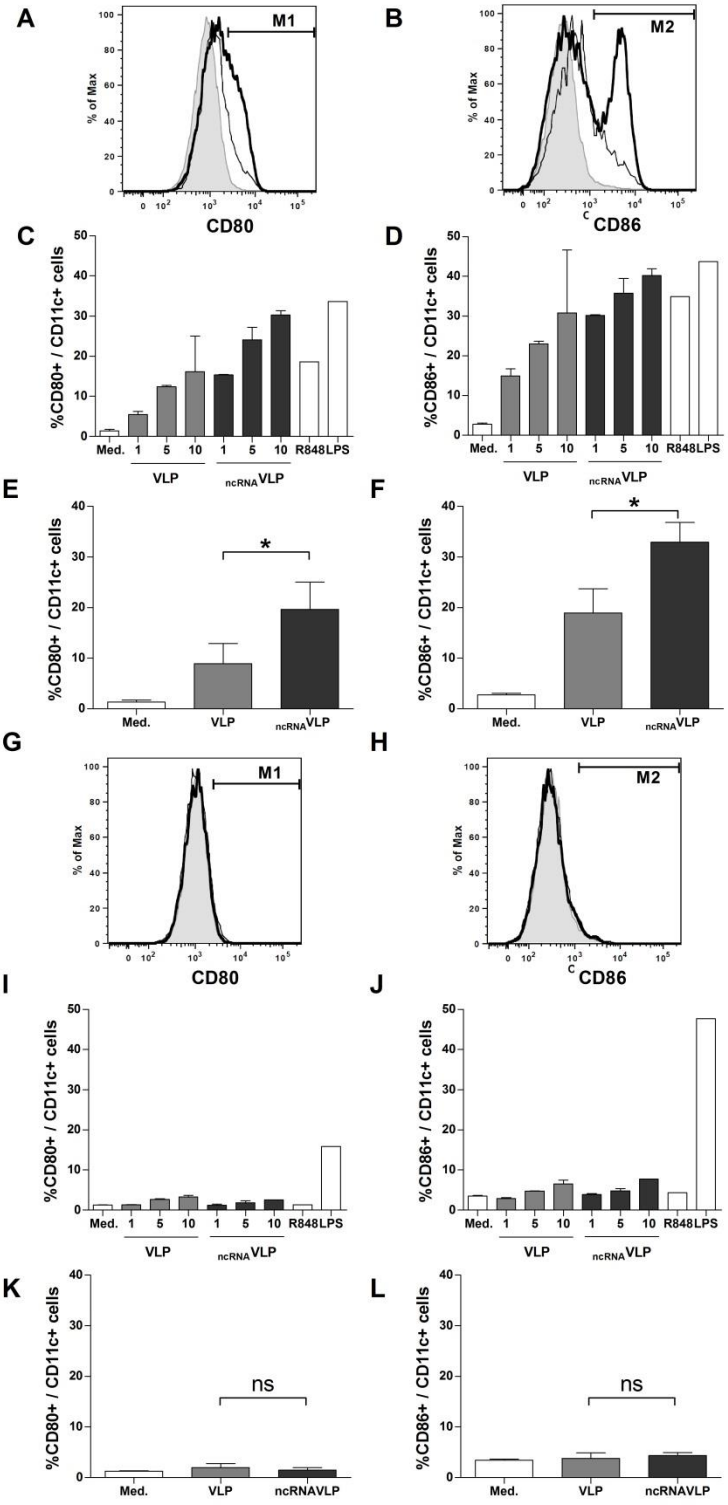

Figure 2:

***In vitro* effect of VLPs carrying or not ncRNA on bone marrow–derived dendritic cell activation.** Immature BMDCs from C57BL/6 **(A-F)** or MyD88$^{-/-}$ **(G-L)** mice were incubated for 24 hours in the presence of 1, 5 or 10 µg/mL of VSV-G pseudotyped MLV-Gag VLPs or $_{ncRNA}$VLPs. CD80 and CD86 expressions were analyzed by flow cytometry. Representative histograms of CD80 **(A, G)** and CD86 **(B, H)** on C57BL/6 BMDCs **(A-B)** or MyD88$^{-/-}$ BMDCs **(G-H)** cultured with 5 µg/mL of VLPs (thin line), $_{ncRNA}$VLPs (thick line) or medium alone (plain histogram) are shown. Related percentages of CD80+ **(C, I)** and CD86+ **(D, J)** were represented. Medium alone, LPS (100 ng/mL) and R848 (1 µg/mL) were used as negative control and two positive controls, respectively. Results represent the mean + SD of duplicates for each dose of VLPs from one experiment representative of two (**C-D, I-J**) and the means +/- SEM of two independent experiments with the dose of 5 µg/mL are represented for CD80 **(E, K)** and CD86 **(F, L)** for C57BL/6 **(E, F)** and MyD88$^{-/-}$ **(K, L)** BMDCs. * $p \leq 0.05$, ns: not significant; Mann-Whitney test.

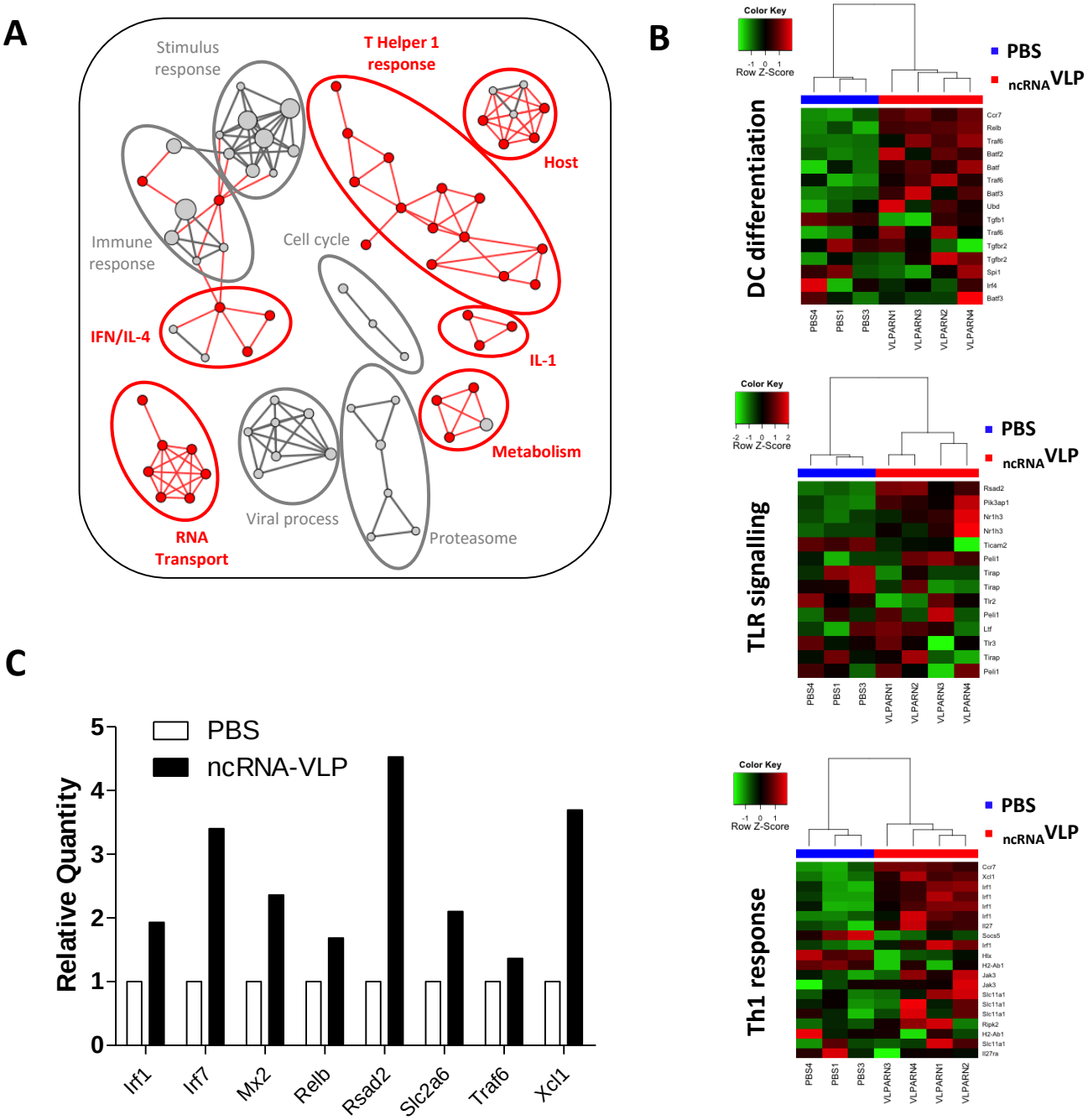

Figure 3:

Transcriptome analysis of splenic dendritic cells after *in vivo* injection of VLPs or $_{ncRNA}$VLPs. Dendritic-specific gene set enrichment analysis using Gene Ontology database signatures allowed us to identify molecular signatures that are differentially enriched in VLP and $_{ncRNA}$VLP groups compared with PBS. **(A)** Results were mapped using Cytoscape software as a network of signatures (nodes) related by similarity (edges). Node size is proportional to the total number of genes in each set. Groups of functionally related signatures are circled and labeled (modules). Grey nodes represent signatures shared between VLP and $_{ncRNA}$VLP groups; red nodes represent signatures that are specific for the $_{ncRNA}$VLP group. FDR q-value = 0.05, P-value = 0.005. **(B)** Heatmap showing three ncRNA-specific signatures. Samples were clustered using a distance-based hierarchical clustering regarding the gene expression. The heatmap colors represent the gene expression (red for high, black for middle, and green for low expression). The Gene Ontology exact names of signatures are “Dendritic cell differentiation” for DC differentiation, “Positive regulation of Toll-Like receptor signaling pathways” for TLR signaling, and “Positive regulation of T helper type 1 immune response” for Th1 response. **(C)** Validation by RT-qPCR of the relative quantity of eight different genes from the three selected signatures.

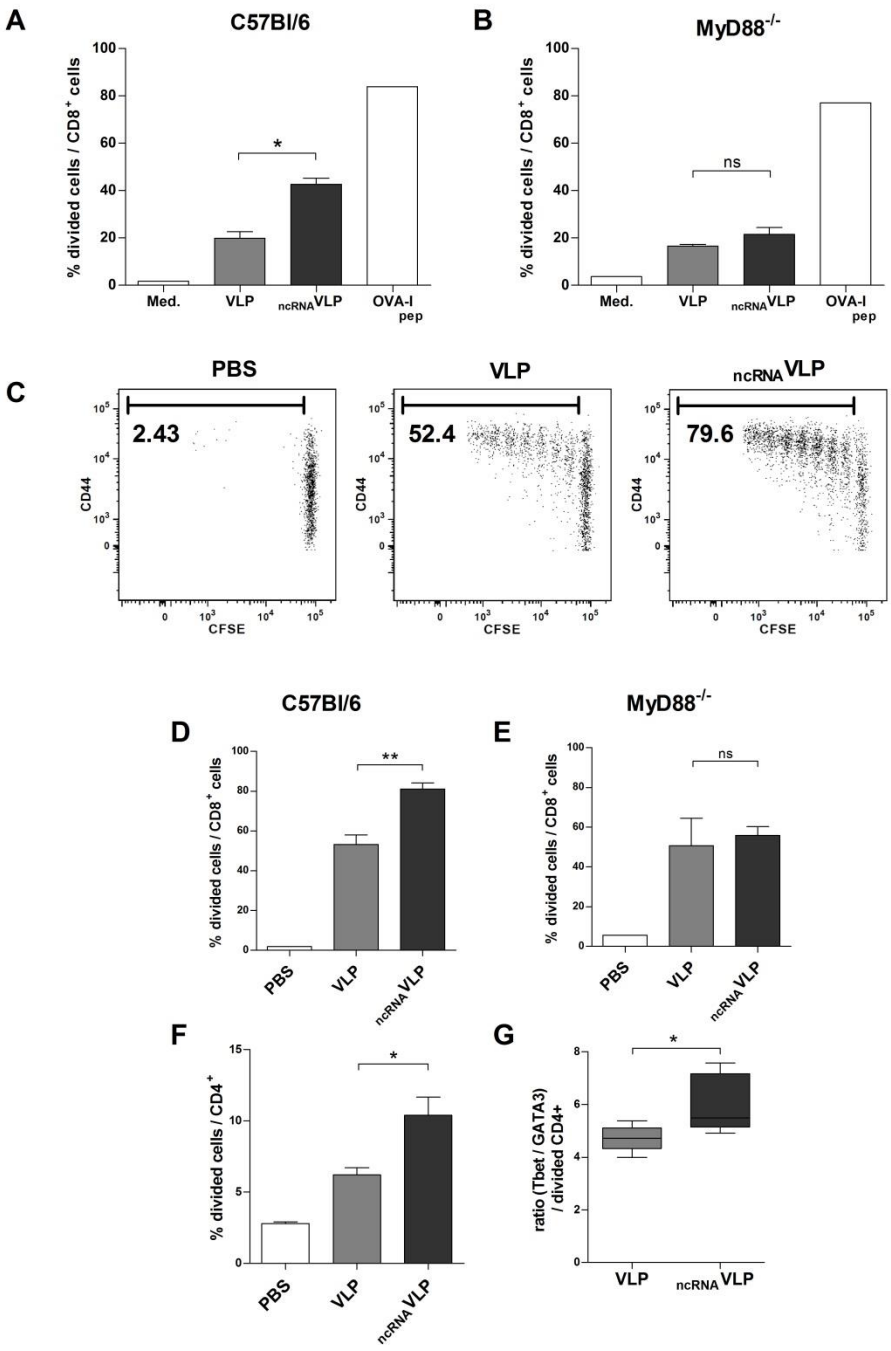

Figure 4:

***In vitro* and *in vivo* effects of VLPs carrying or not ncRNA on T cell proliferation and polarization. (A, B)** *In vitro* proliferation of antigen-specific CD8+ T cells. CFSE-stained OVA-specific OT-I splenic lymphocytes were cultured for 3 days with antigen-presenting cells from C57BL/6 **(A)** or MyD88$^{-/-}$ **(B)** in the presence of 5 µg/mL of VSV-G pseudotyped Gag-OVA VLPs (gray bars) or $_{ncRNA}$VLPs (black bars). Percentages of divided cells were evaluated by flow cytometry analysis of CFSE-low cells among CD8+ Vα2+ live cells. Medium alone and OVA-I peptide were used as negative and positive controls, respectively. Means of triplicates from three independent experiments are shown. **(C-E)** *In vivo* proliferation of antigen-specific CD8+ T cells. C57BL/6 or MyD88$^{-/-}$ mice (n = 5 per group) were injected i.v. with 1 µg of VSV-G pseudotyped Gag-OVA VLPs or $_{ncRNA}$VLPs, and PBS in the control group. Six hours later received 1.5x10^6 CFSE+ OVA-specific CD8+ T cells from OT-I mice. After 3 days, spleens were collected and proliferatiomice n of OVA-specific CD8+ T cells was evaluated by flow cytometry. One representative dot plot of the CFSE profile from each group is depicted in **(C)**. Percentages of divided OVA-specific CD8+ T cells for each dose in C57BL/6 **(D)** and MyD88$^{-/-}$ mice **(E)** are shown. Results represent the mean values +SEM. **(F, G)** *In vivo* proliferation and differentiation of antigen-specific CD4+ T cells. The same experiment as in (**D**) was conducted with OT-II cells instead of OT-I cells. **(F)** Means of the percentage of divided OVA-specific CD4+ T cells and SEM are shown. Geometric means (MFI) ratios of Tbet : GATA3 expression among divided CD4+ T cells are represented in **(G)**. * p ≤ 0.05, ** p≤ 0.01, ns: not significant; Mann-Whitney test.

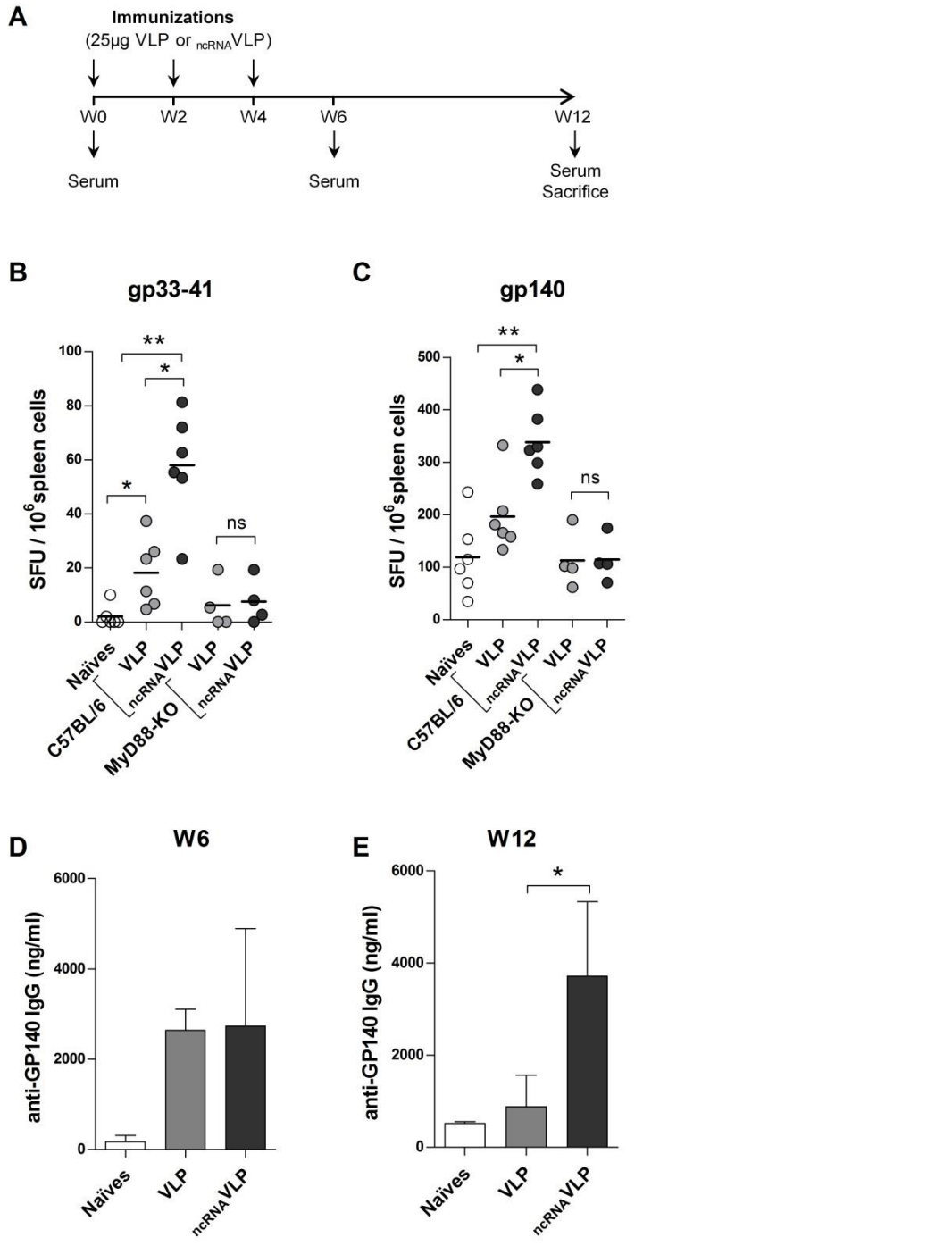

Figure 5:

T- and B-cell immune responses in mice vaccinated with HIV-pseudotyped VLPs carrying or not ncRNA. (A) Schematic representation of the vaccination protocol. C57BL/6 or MyD88-/- mice (n = 5 per group) were immunized 3 times at two-week intervals with 25 µg of HIV-pseudotyped Gag-gp33-41 VLPs or $_{ncRNA}$VLPs. Sera were collected from blood samples at weeks 6 and 12. **(B, C)** Cellular responses were evaluated at week 12 by standard IFN-γ ELISPOT after specific restimulation with either gp33-41 (B) or HIV-gp140 (**C**). Results represent individual values and group means expressed as number of spot forming units (SFUs) per million of splenocytes. **(D, E)** Specific anti-gp140 antibody concentrations were evaluated in serum of immunized or naïve C57BL/6 mice by anti-GP120 ELISA at weeks 6 (**D**) and 12 (**E**). Results represent the mean values + SEM of measured concentrations. * $p \leq 0.05$, ** $p \leq 0.01$; Mann-Whitney test.